

This discussion paper is/has been under review for the journal Atmospheric Chemistry and Physics (ACP). Please refer to the corresponding final paper in ACP if available.

Observation of biogenic secondary organic aerosols in the atmosphere of a mountain site in central China: temperature and relative humidity effects

J. J. Li¹, G. H. Wang¹, J. J. Cao¹, X. M. Wang², and R. J. Zhang³

¹State Key Laboratory of Loess and Quaternary Geology, Institute of Earth Environment, Chinese Academy of Sciences, Xi'an 710075, China

²State Key Laboratory of Organic Geochemistry, Guangzhou Institute of Geochemistry, Chinese Academy of Sciences, Guangzhou 510640, China

³Key Laboratory of Regional Climate-Environment for Temperate East Asia, Institute of Atmospheric Physics, Chinese Academy of Sciences, Beijing 100029, China

Received: 6 May 2013 – Accepted: 17 June 2013 – Published: 4 July 2013

Correspondence to: G. Wang (wanggh@ieecas.cn)

Published by Copernicus Publications on behalf of the European Geosciences Union.

Title Page	Introduction
Abstract	References
Conclusions	Tables
Tables	Figures
◀	▶
◀	▶
Back	Close
Full Screen / Esc	
Printer-friendly Version	
Interactive Discussion	

Abstract

Secondary organic aerosols (SOA) derived from isoprene, pinene and caryophyllene were determined for PM₁₀ and size-segregated (9-stage) aerosols collected at the summit (2060 m, a.s.l.) of Mt. Hua, central China during the summer of 2009. Concentrations of estimated isoprene, α -/ β -pinene and β -caryophyllene derived SOC are 81 ± 53 , 29 ± 14 and $98 \pm 53 \text{ ng m}^{-3}$, accounting for $2.7 \pm 1.0\%$, $0.8 \pm 0.2\%$ and $2.1 \pm 1.0\%$ of OC, respectively. Concentrations of biogenic (BSOA, the isoprene/pinene/caryophyllene oxidation products) and anthropogenic (ASOA, mainly aromatic acids) SOA positively correlated with temperature ($R = 0.57 - 0.90$). However, a decreasing trend of BSOA concentration with an increase in relative humidity (RH) was observed during the sampling period, although a clear trend between ASOA and RH was not found. Based on the AIM Model calculation, we found that during the sampling period an increase in RH resulted in a decrease in the aerosol acidity and thus reduced the effect of acid-catalysis on BSOA formation. Size distribution measurement showed that most of the determined isoprene derived SOA may form in aerosol phase and enriched in the fine mode (< 2.1 μm). 3-Hydroxyglutaric acid, 3-methyl-1,2,3-butanetricarboxylic acid and β -caryophyllinic acid are only presented in fine particles. However, *cis*-pinonic acid presents a large peak in the coarse mode (> 2.1 μm) due to its highly volatile nature.

1 Introduction

Volatile organic compounds (VOCs) produced from the biosphere have a substantial impact on the atmospheric chemistry. On a global scale, biogenic volatile organic compounds (BVOCs, 1150 Tg yr^{-1}), mostly consisting of isoprene, monoterpenes (such as α -/ β -pinene) and sesquiterpenes (such as β -caryophyllene), are one order of magnitude more abundant than anthropogenic VOCs (Guenther et al., 2006). The high emission of BVOCs can significantly increase the occurrence of secondary organic aerosols (SOA) in the atmosphere, which influences the atmospheric radiation budget directly

Temperature and relative humidity effects

J. Li et al.

[Title Page](#)

[Abstract](#)

[Introduction](#)

[Conclusions](#)

[References](#)

[Tables](#)

[Figures](#)

◀

▶

◀

▶

[Back](#)

[Close](#)

[Full Screen / Esc](#)

[Printer-friendly Version](#)

[Interactive Discussion](#)



No other country in the world is as large and diverse a source of aerosols and trace gases as China. Biogenic emission is high in some forested areas of the country. For example, a model study showed that monthly average emission rates of isoprene are more than $30 \text{ mg m}^{-2} \text{ day}^{-1}$ in southeastern, northeastern and central China in summer (Guenther et al., 2006). On the other hand, air pollution in China is serious (Fang et al., 2009; Wang et al., 2006). North China Plain, Guanzhong Basin, and Sichuan Basin in the country are the three most heavily polluted regions in the world, where the annual level of $\text{PM}_{2.5}$ on the ground surface was more than $80 \mu\text{g m}^{-3}$ during 2001–2006 (van Donkelaar et al., 2010). In the past decade, SOA derived from anthropogenic sources in China has been given much attention. However, BSOA in the country has only been documented by a limited number of studies (Fu et al., 2010; Wang et al., 2008; Ding et al., 2011; Hu et al., 2008) with no reports for BSOA from the central part. Atmospheric environment over mountain area is unique because of lower temperature, higher humidity and stronger solar radiation, and thus chemical and physical properties of mountain aerosols differ from those on lowlands (e.g., urban area). Furthermore, mountain area is a receptor for anthropogenic gas and aerosols originating from lowlands by long-range transport. Thus characterizations of alpine BSOA can improve our understanding on physicochemical properties of aerosols in the atmosphere.

In the current paper, we first investigate molecular composition of SOA, including those derived from isoprene, pinene and caryophyllene, in airborne particles at the summit (2060 m altitude) of Mt. Hua in central China and their relationship with temperature and relative humidity (RH), and then measure their size distributions to investigate sources and formation mechanisms of BSOA in the alpine atmosphere.

17645

Temperature and relative humidity effects

J. Li et al.

[Title Page](#)[Abstract](#)[Introduction](#)[Conclusions](#)[References](#)[Tables](#)[Figures](#)[◀](#)[▶](#)[Back](#)[Close](#)[Full Screen / Esc](#)[Printer-friendly Version](#)[Interactive Discussion](#)

2 Experiment section

2.1 Aerosols sampling

Mt. Hua ($34^{\circ}29' \text{ N}$, $110^{\circ}05' \text{ E}$, 2060 m.a.s.l., Fig. 1) is located in the east border of Guanzhong Plain, central China. It is part of the Qin Ling Mountain Range, where around 3000 species of vegetation are known to grow in the region. The low-elevation forests of the foothills are dominated by temperate deciduous trees. At the middle elevations, conifers are mixed with broadleaf birch, oak and hornbeam. However, sub-alpine forests of fir, cunninghamia, and birch are dominated at high-elevation forests (http://en.wikipedia.org/wiki/Qin_Ling). Collections of PM_{10} and size-segregated particles were simultaneously performed at the summit of Mt. Hua during the summer of 2009 (15 July ~ 25 August). A medium-volume air sampler (KC-120H, made in China) was operated for PM_{10} collection at an airflow rate of 100 L min^{-1} . Size-segregated samples were collected using an Andersen 9-stage air sampler (Thermo electronic Company, USA) with the cutoff points at 9.0, 5.8, 4.7, 3.3, 2.1, 1.1, 0.7, and $0.4 \mu\text{m}$ under an airflow rate of 28.3 L min^{-1} . A total of 34 PM_{10} samples were collected each lasting for 24 h. The size-resolved aerosols (9 samples per set, 3 sets) were collected for 5–6 days in each set. All samples were collected on pre-baked (450°C for 8 h) quartz microfiber filters (Whatman 42). After sampling, the filter was sealed in an aluminum bag and stored at -18°C prior to analysis. Three field blank samples were collected before and after sampling by mounting the filters onto the sampler for about 10 min without sucking any air.

2.2 Sample extraction, derivatization and GC/MS quantification

Detailed methods for extraction, derivatization and gas chromatography/mass spectrometry (GC/MS) analysis were described elsewhere (Wang et al., 2006, 2009). Briefly, one fourth of the sample/blank filter was cut in pieces and extracted with a mixture of dichloromethane and methanol (2 : 1, v/v) under ultrasonication (3 times and

Temperature and relative humidity effects

J. Li et al.

Title Page

Abstract

Introduction

Conclusions

References

Tables

Figures

◀

▶

◀

▶

Back

Close

Full Screen / Esc

Printer-friendly Version

Interactive Discussion



15 min per time). The extracts were concentrated using a rotary evaporator under a vacuum condition and then blown down to dryness using pure nitrogen. After reaction with a mixture of N,O-bis-(trimethylsilyl) trifluoroacetamide (BSTFA) and pyridine (5 : 1, v/v) at 70 °C for 3 h, the derivatives were determined using a GC/MS technique below.

Gas chromatography–mass spectrometry (GC/MS) analysis of the derivatized fraction was performed using an Agilent 7890A GC coupled with an Agilent 5975C MSD. The GC separation was carried out on a DB-5MS fused silica capillary column with the GC oven temperature programmed from 50 °C (2 min) to 120 °C at 15 °C min⁻¹ and then to 300 °C at 5 °C min⁻¹ with a final isothermal holds at 300 °C for 16 min. The sample was injected in a splitless mode at an injector temperature of 280 °C, and scanned from 50 to 650 Daltons using electron impact (EI) mode at 70 eV. Detailed chemical characterization and possible sources of the 15 detected organic compounds in this study are listed in Table 1. In addition, GC/MS response factors of *cis*-pinonic acid, succinic acid, glutaric acid, malic acid, phthalic acids, levoglucosan and arabitol were determined using authentic standards, while GC/MS response factors of 2-methylglyceric acid (MGA), 2-methyltetrols (MT/ME), 3-hydroxyglutaric acid (HGA), 3-methyl-1,2,3-butanetricarboxylic acid (MBTCA) and β -caryophyllinic acid (PA) were replaced by those of glyceric acid, erythritol, tartaric acid, suberic acid and *cis*-pinic acid, because the authentic standards are not commercially available. Average recoveries of the target compounds were better than 70 %. No significant contamination (< 10 % of those in the samples) was found in the blanks. Data presented were corrected for the field blanks but not corrected for the recoveries.

OC and EC in the PM₁₀ samples were analyzed using DRI Model 2001 Carbon analyzer following the Interagency Monitoring of Protected Visual Environments (IM-PROVE) thermal/optical reflectance (TOR) protocol (Chow et al., 2004). Inorganic ions including SO₄²⁻, NO₃⁻ and NH₄⁺ in PM₁₀ and size-resolved samples were analyzed using ion chromatography (Li et al., 2011; Shen et al., 2008). Particle in-situ pH (pH_{IS}) and aerosol liquid water content (LMC) were calculated by Aerosol Inorganic Model (AIM) using a SO₄²⁻-NO₃⁻-NH₄⁺-H⁺ system (AIM-II) (Clegg et al., 1998a,b)

3 Results and discussion

3.1 Abundance of OC, EC and SOA in PM₁₀

5 3.1.1 Overall results

Concentrations of detected organic compounds, OC, EC and inorganic ions are summarized in Table 2. PM₁₀, OC and EC concentrations at Mt. Hua in summer were 43 ± 17 , 3.5 ± 1.3 and $0.65 \pm 0.27 \mu\text{g m}^{-3}$, respectively, and lower than those in winter (54 ± 24 , 5.9 ± 2.5 and $0.9 \pm 0.6 \mu\text{g m}^{-3}$) (Li et al., 2012) mainly due to decreased emissions of biomass and coal burning for house heating. However, the favorable meteorological conditions (i.e., higher temperature and RH, and increased boundary layer height) resulted in higher concentrations of SO₄²⁻ and NH₄⁺ (21 ± 12 and $4.3 \pm 2.5 \mu\text{g m}^{-3}$, respectively) in summer compared to those (5.8 ± 3.6 and $1.6 \pm 0.9 \mu\text{g m}^{-3}$, respectively) in winter (Li et al., 2011).

15 Three compounds were determined as oxidation products of isoprene in the PM₁₀ samples, which are 2-methylglyceric acid (MGA, $4.1 \pm 2.2 \mu\text{g m}^{-3}$), 2-methylthreitol (MT, $3.6 \pm 2.8 \mu\text{g m}^{-3}$) and 2-methylerythritol (ME, $4.9 \pm 3.6 \mu\text{g m}^{-3}$) (Table 2). *cis*-Pinonic acid (PA), 3-hydroxyglutaric acid (HGA) and 3-methyl-1,2,3-butanetricarboxylic acid (MT-BCA) are the major photooxidized products of α -/ β -pinene, and their concentrations are 3.0 ± 1.4 , 2.1 ± 1.1 and $1.6 \pm 1.1 \mu\text{g m}^{-3}$, respectively. β -Caryophyllinic acid, one of β -caryophyllene (a sesquiterpene) oxidation products, was also determined in this study, and its concentration is $2.2 \pm 1.2 \mu\text{g m}^{-3}$. Contributions of BVOCs to secondary organic carbon (SOC) in the atmosphere of Mt. Hua were estimated using a tracer-based method reported by Kleindienst et al. (2007). Concentrations of estimated isoprene, α -

Title Page

Abstract

Introduction

Conclusions

References

Tables

Figures

◀

▶

◀

▶

Back

Close

Full Screen / Esc

Printer-friendly Version

Interactive Discussion



/ β -pinene and β -caryophyllene derived SOC are 81 ± 53 , 29 ± 14 and $98 \pm 53 \text{ ng C m}^{-3}$, accounting for $2.7 \pm 1.0\%$, $0.8 \pm 0.2\%$ and $2.1 \pm 1.0\%$ of OC, respectively.

Succinic, glutaric and malic acids in the atmosphere are produced mainly by photochemical reactions of unsaturated hydrocarbons and fatty acids from biomass burning and coal combustion (Kawamura and Yasui, 2005; Wang et al., 2010). Concentrations ($2.2\text{--}5.8 \text{ ng m}^{-3}$) of these compounds in the Mt. Hua PM₁₀ samples are comparable to the BSOA above. Phthalic acids are derived from photooxidation of polycyclic aromatic hydrocarbons (PAHs) (Wang et al., 2007; Simoneit et al., 2004b), and pyrolysis of plastic materials (Kawamura and Pavuluri, 2010). Their concentrations in the Mt. Hua samples are $0.16\text{--}4.9 \text{ ng m}^{-3}$. Levoglucosan and arabitol are tracers of biomass burning and biological emissions, respectively (Simoneit et al., 2004a; Engling et al., 2009). Levoglucosan is lower in summer ($14 \pm 12 \text{ ng m}^{-3}$) than in winter ($65 \pm 30 \text{ ng m}^{-3}$), in contrast to arabitol ($5.5 \pm 3.5 \text{ ng m}^{-3}$ in summer and $3.0 \pm 2.0 \text{ ng m}^{-3}$ in winter), which is higher in summer (Li et al., 2012), indicating a decreased biomass burning and an increased biogenic activity in the hot season.

3.1.2 Comparison between different air masses classified by back-trajectories analysis

As shown in Fig. 1, air masses reaching the sampling site during the campaign were from three directions: southerly, easterly and northerly. Thus, concentrations of total detected compounds, temperatures and RH during the summer campaign are categorized into the three groups (Table 2). Although PM₁₀ concentration ($46 \pm 6.6 \mu\text{g m}^{-3}$, Table 2) from northerly is slightly higher than those ($42 \pm 17 \mu\text{g m}^{-3}$, Table 2) from the southerly and easterly, SO₄²⁻, NH₄⁺ and *o*-phthalic acid in the samples showed higher concentrations when air mass was transported from the south and east directions, indicating more anthropogenic pollutants in these regions. As shown in Table 2, nearly all the BSOA tracers presented higher concentrations for the southerly and easterly samples than those for the northerly samples, which is reasonable as plant vegeta-

Title Page	Abstract	Introduction
Conclusions	References	
Tables	Figures	
◀	▶	
◀	▶	
Back	Close	
Full Screen / Esc		
Printer-friendly Version		
Interactive Discussion		



tion is much more abundant in southern and eastern China (Guenther et al., 2006). Furthermore, the higher concentration of SO_4^{2-} and NO_3^- can also enhance the BSOA formation by an acid-catalyzed reaction (Surratt et al., 2010).

3.1.3 Comparison of BSOA tracers with other studies

- 5 A comparison of concentration and diagnostic ratio of isoprene, α -/ β -pinene and β -caryophyllene products was shown in Table 3. In this study, aerosol samples are collected at a summit of Mt. Hua (2060 m a.s.l.), where vegetation is very limited and the ground surfaces are mostly rocks. Thus, BSOA tracers present lowest concentration in the elevated region than those in other areas except Alert (82.5° N, 62.3° W)
- 10 in the Canadian High Arctic. All the tracers at the Alert site are 1–3 orders of magnitude lower than those in other regions. 2-Methyltetros (sum of 2-methylthreitol and 2-methylerythritol) are the major products of isoprene (Kleindienst et al., 2006; Edney et al., 2005; Claeys et al., 2010), thus their contribution to organic carbon of airborne particles can be used to roughly compare the variation of isoprene emission. The ratios
- 15 present a decreasing trend along with an increase in latitude, highest at the equatorial region (Balbina, Brazil, 1.8%) (Claeys et al., 2004) and lowest at the Arctic site (Alert, Canada 0.019 %) (Fu et al., 2009). The carbon contribution of 2-methyltros in Mt. Hua ($0.11 \pm 0.06\%$) is lower than those (0.17–0.75 %, Table 3) in other Chinese regions excluding Wangqingsha and Chongming, which can be explained by lower levels
- 20 of biogenic precursors due to less abundant vegetation in central and western China compared to the eastern part of the country (Guenther et al., 2006). However, the lowest ratios in Wangqingsha (0.070 %) and Chongming (0.020 %) most likely resulted from the high anthropogenic OC input since both sites are close to the urban areas.

25 MBTCA is aged biogenic product from gas-phase oxidation of *cis*-pinonic acid (PA) by OH (Szmigielski et al., 2007; Henry and Donahue, 2012). Thus the ratio of MBTCA/PA ($R_{\text{MBTCA/PA}}$) is indicative of aerosol ageing (Kulmala et al., 2011). The ratios (0.54 and 1., Table 3) at Mt. Hua and Mt. Tai are higher than that (0.32, Table 3) at Wangqingsha, a lowland rural site in southern China, indicating the mountain aerosols

Title Page	
Abstract	Introduction
Conclusions	References
Tables	Figures
◀	▶
◀	▶
Back	Close
Full Screen / Esc	
Printer-friendly Version	
Interactive Discussion	



Temperature and relative humidity effects

J. Li et al.

are more oxidized. Such a phenomenon may be related to the stronger mountaintop radiation that causes the BSOA being highly oxidized. Averaged ratios of MBTCA/PA ratios are 0.71 ± 0.27 , 0.43 ± 0.31 and 0.29 ± 0.12 for the southerly, easterly and northerly samples, respectively, indicating that aerosols derived from the southerly air masses were more aged. The Mexico Campaign reported that MBTCA/PA (4.8, Table 3) in the rural area is nearly 5 times higher than that (0.91) in urban region due to more aged BSOA (Stone et al., 2010), which is consistent with the larger contributions ($25 \pm 5\%$) of aged low-MW acids (mainly oxalic acid) to WSOC at the peripheral rural site than that at urban site ($8.2 \pm 3.4\%$) (Stone et al., 2010). Concentration of MBTCA at the Arctic site is almost one order of magnitude higher than PA ($R_{MBTCA/PA} = 9.4$ at Alert, Table 3). Such a spatial variation in the ratios demonstrates a continuous oxidation of BSOA during transport.

3.2 Calculations of particle in-situ pH and liquid water content

Chemical reactions in aerosol phase or gas-particle distributions in aerosol surface are much linked to the actual pH (i.e., in-situ pH, pH_{IS}) in the aqueous phase and liquid water content (LWC) of particles (Xue et al., 2011). Thus, aerosol in-situ pH and liquid water content are calculated in this study using the following equation:

$$pH_{IS} = -\log \alpha_{H^+} = -\log(\gamma_{H^+} \times n_{H^+} \times 1000/V_a) \quad (1)$$

Where α_{H^+} is activity of H^+ in mol L^{-1} in the aqueous phase on the particle, γ_{H^+} is the activity coefficient of H^+ , n_{H^+} is free H^+ in the unit of mol m^{-3} of air, and V_a is volume concentration of the aqueous phase of aerosol in ambient atmosphere in the unit of $\text{cm}^3 \text{m}^{-3}$. γ_{H^+} , n_{H^+} and V_a as well as LWC ($\mu\text{mol m}^{-3}$) are derived using Aerosol Inorganic Model (AIM) (Clegg et al., 1998b,a). As SO_4^{2-} , NO_3^- and NH_4^+ are detected in this study, we chose AIM-II model for calculation, which considers a SO_4^{2-} - NO_3^- - NH_4^+ - H^+ system and allows variable temperature and relative humidity. As shown in Table 2, pH_{IS} are -0.08 ± 0.64 in PM_{10} at Mt. Hua, which is comparable with those in $\text{PM}_{2.5}$ samples in Hong Kong (-0.08 ± 0.81 during the summer of

Title Page	
Abstract	Introduction
Conclusions	References
Tables	Figures
◀	▶
◀	▶
Back	Close
Full Screen / Esc	
Printer-friendly Version	
Interactive Discussion	



Title Page

Abstract

Introduction

Conclusions

References

Tables

Figures

◀

▶

◀

▶

Back Close

Full Screen / Esc

Printer-friendly Version

Interactive Discussion



2009) (Xue et al., 2011) but higher than those at Qinghai Lake (-1.20 ± 0.32 during the summer of 2010) (Li et al., 2013), a highland site with a distance of around 1000 km west to Mt. Hua. It is worth noting that in-situ acidity of the Mt. Hua PM₁₀ samples may be somewhat overestimated due to the relatively higher level of mineral ions (e.g., Ca²⁺ and Mg²⁺) in the samples, which were not included by the model. LWC of PM₁₀ at Mt. Hua are $4.87 \pm 4.90 \mu\text{mol m}^{-3}$, and much larger than those of PM_{2.5} in Hong Kong ($0.39 \pm 0.12 \mu\text{mol m}^{-3}$) (Xue et al., 2011), probably suggesting that the mountain aerosols are more hygroscopic.

3.3 Effects of temperature on BSOA formation

Temporal variations of BSOA tracers, OC and EC in PM₁₀ and meteorological conditions are shown in Fig. 3. The sharp declines during the rainy days suggest a significant scavenging effect of wet deposition. The variation of the seven BSOA tracers exhibits the same pattern, because they are formed via similar pathways.

The relationships between BSOA and meteorological parameters are plotted in Fig. 4a–l according to the three different classes of air masses. Nearly all of the detected BSOA tracers showed a robust linear relation with ambient temperature, largely due to enhancements in BVOCs emission and BSOA production under higher temperature. However, the temperature dependence of gas-particle partitioning of the compounds may be relatively weaker. For example, the temperature dependence of gas-particle partitioning of pinonic acid, a highly volatile compound, can be approximated by an Arrhenius activation energy of $\sim 0.21 \text{ kJ mol}^{-1}$ (Zhang et al., 2010). Such a temperature dependence is also observed in other areas, such as in the central Pearl River Delta region, Southern China (except MGA) (Ding et al., 2011) and Research Triangle Park, North Carolina, USA (Offenberg et al., 2011). As shown in Fig. 4b, the slopes of 2-methyltetrosols in this study are 2.7, 2.0 and 0.79 for the PM₁₀ samples from southerly, easterly and northerly air masses, respectively, much lower than that (5.27) (Ding et al., 2011) in southern China. This can be explained by a higher isoprene emission due to

more abundant vegetation in the south lowland region (Guenther et al., 2006). The slopes of the regression equation in the southerly and easterly air masses are higher than those from northerly, which is consistent with plant abundance distributions in the three regions.

5 3.4 Effects of relative humidity on BSOA formation

As far as we know, field observations of the influence of relative humidity (RH) on SOA formation from biogenic VOCs were documented in very limited number. Some chamber studies explored the effects of humidity on BSOA production. For example, Zhang et al. (2011) conducted a chamber study and found that 2-methylglyceric acid and its corresponding oligomers were enhanced in the particle-phase under lower RH condition, in contrast, the 2-methyltetrosols did not substantially vary under different RH conditions. However, in this study we found that all of the detected isoprene, α -/ β -pinene and β -caryophyllene showed a significant negative linear correlation with relative humidity (Fig. 4g–l).

In fact, an enhancement effect of aerosol acidity on BSOA formation was found by several chamber and field studies (Ding et al., 2011; Iinuma et al., 2004; Offenberg et al., 2009). Surratt et al. (2010) found that isoprene epoxydiols (IEPOX) are key intermediates of SOA formation from isoprene under low NO_x condition, which are initially formed in the gas-phase and subsequently partitioned into aerosol aqueous-phase.

The aerosol phase IEPOX further convert to 2-methyltetrosols (MT/ME) and C₅-alkene triols, the three most common SOA of isoprene, by an acid-catalyzed ring opening of this epoxydiol and a subsequent nucleophilic addition. Lin et al. (2012) again confirmed that IEPOX reactively uptake onto acidified sulfate aerosols to produce MT and ME as well as other IEPOX-derived SOA tracers, including the C₅-alkene triols, 3-methyltetrahydrofuran-3,4-diols, dimers, and organosulfates. However, aerosol in-situ acidity is strongly dependent on relative humidity. Based on the AIM model calculations, we found that relative humidity (RH) of the mountaintop atmosphere exhibits a robust linear correlation with the in-situ pH (pH_{IS}) of the PM₁₀ particles ($R^2 = 0.95$)

[Title Page](#)

[Abstract](#)

[Introduction](#)

[Conclusions](#)

[References](#)

[Tables](#)

[Figures](#)

◀

▶

[Back](#)

[Close](#)

[Full Screen / Esc](#)

[Printer-friendly Version](#)

[Interactive Discussion](#)



and a moderate correlation with liquid water content of the particles ($R^2 = 0.64$). As shown in Fig. 4m–o, all the calculated SOC concentrations showed significant negative linear correlations with pH_{IS} , suggesting that the suppressed effect of RH on BSOA formation is most likely related to reducing aerosol acidity. Similar researches have been performed in the southeastern United States although the AIM model for most samples did not work due to the aerosol either being fully neutralized or the RH being too low in the region (Lin et al., 2013b; Budisulistiorini et al., 2013). Interestingly, Budisulistiorini et al. (2013) found that the IEPOX-OA factor obtained by PMF (positive matrix factorization) analysis of ACSM (Aerosol Chemical Speciation Monitor) data also shows a moderate correlation ($R^2 = 0.25$) with in situ acidity of particles.

Moreover, Zhang et al. (2011) reported that low RH circumstance can improve BSOA yields by promoting particle phase organic esterification process. Nguyen et al. (2011) also pointed out that the suppression of condensation and addition reactions are the most important chemical effects of the increased RH on BSOA formation. However, we found there were no clear correlation between biogenic SOC (BSOC) concentrations and liquid water content (LWC) of the particles (Fig. 4p–r). High LWC is favorable for a conversion of BSOA precursors into aqueous phase and thus enhances BSOA production. On the other hand, however, high LWC may reduce particle acidity, which is unfavorable for BSOA production. Moreover, the effect of RH on precursor emission strength may be another potential factor influencing the BSOA production. In any case, more chamber and field studies are warranted to conduct for understanding the exact mechanism of effect of RH on BSOA formation.

Phthalic acids may be produced by the oxidation of naphthalene and other polycyclic aromatic hydrocarbons (Kawamura et al., 2005; Kawamura and Ikushima, 1993). Similar to BSOA formation, these anthropogenically derived SOA also showed a positive relation with temperature ($R > 0.6$). A clear correlation between RH and concentration of phthalic acids was not observed in this study ($R < 0.1$, $p > 0.7$). However, recent investigations indicated that the yields of SOA derived from some aromatic compounds (such as xylenes and toluene) positively correlated with the particle water content (Ka-

Temperature and relative humidity effects

J. Li et al.

[Title Page](#)

[Abstract](#)

[Introduction](#)

[Conclusions](#)

[References](#)

[Tables](#)

[Figures](#)

◀

▶

◀

▶

[Back](#)

[Close](#)

[Full Screen / Esc](#)

[Printer-friendly Version](#)

[Interactive Discussion](#)



mens et al., 2011; Zhou et al., 2011), emphasizing the important impact of liquid water content in the particles (RH depended) on anthropogenic SOA formation.

3.5 Size distribution

To further discuss the source and formation mechanism of the BSOA in the mountain atmosphere, detailed information of their size distribution was investigated. Table 5 shows the concentration and geometric mean diameters (GMD) of the detected organic compositions and inorganic ions in fine ($< 2.1 \mu\text{m}$) and coarse ($> 2.1 \mu\text{m}$) modes, and their concentrations as a function of size are plotted in Fig. 5.

2-Methyltetrosols present a unimodal size distribution pattern with a peak at the size of 0.7–1.1 μm (Fig. 5b). As mentioned above, IEPOX are key intermediates of isoprene oxidation products of 2-methyltetrosols under low- NO_x condition through heterogeneous reactions in aerosol-phase (Surratt et al., 2010; Lin et al., 2012). In contrast, MGA is formed via nucleophilic attack of water on the oxirane ring of 2-methyloxirane-2-carboxylic acid (methacrylic acid epoxide, MAE), which is produced by isoprene oxidation under high- NO_x condition (Lin et al., 2013a). MGA in the Mt. Hua aerosols present a bimodal size distribution pattern with a major peak in the fine mode ($< 2.1 \mu\text{m}$) and a minor peak in the coarse mode ($> 2.1 \mu\text{m}$) (Fig. 5a).

cis-Pinonic acid (PA) exhibits a bimodal pattern with a large peak in the coarse mode ($> 2.1 \mu\text{m}$) (Fig. 5c), in contrast to HGA and MBTCA, which only present in the fine mode (Fig. 5d and e). Such distributions are consistent with those in Mainz, Germany (Zhang et al., 2010). PA is formed by a gas-phase oxidation of pinene with ozone and a subsequent adsorption onto pre-existing particles (Hallquist et al., 2009). On the contrary, MBTCA is likely formed in the gas phase by further reactions of *cis*-pinonic acid or *cis*-pinic acid involving participation of OH radical (Jaoui et al., 2005; Szmigelski et al., 2007). The differences in size distributions of PA and MBTCA can be ascribed to the highly volatile nature of *cis*-pinonic acid. Zhang et al. (2010) pointed out that *cis*-pinonic acid predominantly present in the gas phase. Coarse particle are generally basic, because they are in most cases enriched with mineral species. Therefore, *cis*-

Title Page	
Abstract	Introduction
Conclusions	References
Tables	Figures
◀	▶
◀	▶
Back	Close
Full Screen / Esc	
Printer-friendly Version	
Interactive Discussion	



Temperature and relative humidity effects

J. Li et al.

pinonic acid in gas-phase may prefer to reactively uptake onto coarse particles. Only a fine mode of β -caryophyllinic acid (CA) was observed in the mountain atmosphere (Fig. 5f).

Succinic (C_4^{di}) and glutaric (C_5^{di}) acids are formed mostly from anthropogenic volatile organic compounds, which are firstly oxidized as gaseous keto-carboxylic acids and then partitioned into particle phase followed by a further oxidation as the dicarboxylic acids (Wang et al., 2011), thus both present a bimodal size distribution (Fig. 5g and h). On the contrary, malic acid is found to be mostly produced in biomass combustion process and emitted into the air as fine particles (Wang et al., 2011, 2012), thus malic acid showed the fine mode pattern (Fig. 5i). *o*-Phthalic acid is formed via a gaseous oxidation of naphthalene and followed by a subsequent adsorption/condensation onto pre-existing particles, thus, showed a bimodal pattern (Fig. 5j), in contrast to a unimodal pattern of *p*-phthalic acid (Fig. 5l), which is largely formed by a pyrolysis of plastic materials and emitted into the air as fine particles (Wang et al., 2012). Levoglucosan, a key tracer for biomass burning, presents a unimodal distributing, peaking at a size of 0.7–1.1 μm in summer (Fig. 5m). In contrast, arabitol is dominated in coarse particle as it mostly originates from pollen, spore and other biota (Fig. 5n). SO_4^{2-} and NH_4^+ are dominated in the fine mode (Fig. 5o and q), similar to those in winter (Li et al., 2011). However, coarse particles in the mountain atmosphere are more significantly enriched in NO_3^- compared to that in Xi'an (unreported data), a mega-city near Mt. Hua (Fig. 5p). Such a shift to large particles is caused by an evaporation of nitrate from fine particles and a subsequent adsorption onto coarse particles during the air mass transport onto the mountaintop.

4 Summary and conclusion

²⁵ BSOA derived from isoprene, pinene and sesquiterpene were determined for PM₁₀ and size-resolved aerosols collected at the mountaintop of Mt. Hua. Back-trajectories analysis showed that all the BSOA tracers present higher concentrations in the sam-

17656



Temperature and relative humidity effects

J. Li et al.

Title Page

Abstract

Introduction

Conclusions

References

Tables

Figures



Back

Close

Full Screen / Esc

Printer-friendly Version

Interactive Discussion



plexes from the southerly and easterly than in those from the northerly, indicating higher BVOC emissions and/or more BSOA production. Concentrations of the BSOA in the mountain samples increased with an increase in temperature during the campaign, because higher temperature is favorable for BVOCs emission and subsequent oxidation.
5 In contrast, RH showed significant linear negative correlations with concentrations of all the isoprene, pinene and caryophyllene products. Based on the AIM model calculation, we found that an increase in RH can result in a decrease in particle in-situ acidity, which reduces the effect of acid-catalysis on BSOA formation. However, such a significant relation was not observed for LWC and BSOA. Size distribution details
10 were also explored for the target compounds. Most of the BSOA is enriched in the fine mode (< 2.1 µm) except for PA, which is dominated in the coarse mode (> 2.1 µm) due to its highly volatile nature. Size distributions of levoglucosan, arabitol and other secondary aerosols were also investigated. These size distribution details are helpful for recognizing their atmospheric fate including formation, adsorption and evaporation.

15 **Acknowledgements.** This work was financially supported by the “Strategic Priority Research Program” of the Chinese Academy of Sciences (Grant No. XDA05100103, XDB05020401), and the Ministry of Science & Technology of China (2007BAC30B00, 2012BAH31B00). We also thank the AIM Model group for using the AIM model.

References

- 20 Budisulistiorini, S. H., Canagaratna, M. R., Croteau, P. L., Marth, W. J., Baumann, K., Edgerton, E. S., Shaw, S. L., Knipping, E. M., Worsnop, D. R., Jayne, J. T., Gold, A., and Suratt, J. D.: Real-time continuous characterization of secondary organic aerosol derived from isoprene epoxydiols in Downtown Atlanta, Georgia, using the aerodyne aerosol chemical speciation monitor, Environ. Sci. Technol., 47, 5686–5694, doi:10.1021/es400023n, 2013.
- 25 Chow, J. C., Watson, J. G., Chen, L. W. A., Arnott, W. P., and Moosmuller, H.: Equivalence of elemental carbon by thermal/optical reflectance and transmittance with different temperature protocols, Environ. Sci. Technol., 38, 4414–4422, doi:10.1021/es034936u, 2004.

Temperature and
relative humidity
effects

J. Li et al.

- Claeys, M., Graham, B., Vas, G., Wang, W., Vermeylen, R., Pashynska, V., Cafmeyer, J., Guyon, P., Andreae, M. O., Artaxo, P., and Maenhaut, W.: Formation of secondary organic aerosols through photooxidation of isoprene, *Science*, 303, 1173–1176, 2004.
- 5 Claeys, M., Kourtchev, I., Pashynska, V., Vas, G., Vermeylen, R., Wang, W., Cafmeyer, J., Chi, X., Artaxo, P., Andreae, M. O., and Maenhaut, W.: Polar organic marker compounds in atmospheric aerosols during the LBA-SMOCC 2002 biomass burning experiment in Rondônia, Brazil: sources and source processes, time series, diel variations and size distributions, *Atmos. Chem. Phys.*, 10, 9319–9331, doi:10.5194/acp-10-9319-2010, 2010.
- 10 Clegg, S. L., Brimblecombe, P., and Wexler, A. S.: Thermodynamic model of the system $\text{H}^+ \text{-NH}_4^+ \text{-Na}^+ \text{-SO}_4^{2-} \text{-NB}_3^- \text{-Cl}^- \text{-H}_2\text{O}$ at 298.15 K, *J. Phys. Chem. A*, 102, 2155–2171, doi:10.1021/jp973043j, 1998a.
- 15 Clegg, S. L., Brimblecombe, P., and Wexler, A. S.: Thermodynamic model of the system $\text{H}^+ \text{-NH}_4^+ \text{-SO}_4^{2-} \text{-NO}_3^- \text{-H}_2\text{O}$ at tropospheric temperatures, *J. Phys. Chem. A*, 102, 2137–2154, doi:10.1021/jp973042r, 1998b.
- 20 Ding, X., Wang, X.-M., and Zheng, M.: The influence of temperature and aerosol acidity on biogenic secondary organic aerosol tracers: observations at a rural site in the central Pearl River Delta region, South China, *Atmos. Environ.*, 45, 1303–1311, 2011.
- 25 Edney, E. O., Kleindienst, T. E., Jaoui, M., Lewandowski, M., Offenberg, J. H., Wang, W., and Claeys, M.: Formation of 2-methyl tetrosols and 2-methylglyceric acid in secondary organic aerosol from laboratory irradiated isoprene/ NO_x/SO_2 /air mixtures and their detection in ambient $\text{PM}_{2.5}$ samples collected in the eastern United States, *Atmos. Environ.*, 39, 5281–5289, doi:10.1016/j.atmosenv.2005.05.031, 2005.
- Engling, G., Lee, J. J., Tsai, Y. W., Lung, S. C. C., Chou, C. C. K., and Chan, C. Y.: Size-resolved anhydrosugar composition in smoke aerosol from controlled field burning of rice straw, *Aerosol Sci. Tech.*, 43, 662–672, doi:10.1080/02786820902825113, 2009.
- Fang, M., Chan, C. K., and Yao, X. H.: Managing air quality in a rapidly developing nation: China, *Atmos. Environ.*, 43, 79–86, doi:10.1016/j.atmosenv.2008.09.064, 2009.
- 30 Froyd, K. D., Murphy, S. M., Murphy, D. M., de Gouw, J. A., Eddingsaas, N. C., and Wennberg, P. O.: Contribution of isoprene-derived organosulfates to free tropospheric aerosol mass, *P. Natl. Acad. Sci. USA*, 107, 21360–21365, doi:10.1073/pnas.1012561107, 2010.

Title Page	
Abstract	Introduction
Conclusions	References
Tables	Figures
	
	
Back	Close
Full Screen / Esc	
Printer-friendly Version	
Interactive Discussion	



Temperature and
relative humidity
effects

J. Li et al.

Title Page

Abstract

Introduction

Conclusions

References

Tables

Figures

◀

▶

Back

Close

Full Screen / Esc

Printer-friendly Version

Interactive Discussion



Fu, P. Q., Kawamura, K., Chen, J., and Barrie, L. A.: Isoprene, monoterpene, and sesquiterpene oxidation products in the high arctic aerosols during late winter to early summer, *Environ. Sci. Technol.*, 43, 4022–4028, doi:10.1021/es803669a, 2009.

Fu, P. Q., Kawamura, K., Kanaya, Y., and Wang, Z. F.: Contributions of biogenic volatile organic compounds to the formation of secondary organic aerosols over Mt Tai, Central East China, *Atmos. Environ.*, 44, 4817–4826, doi:10.1016/j.atmosenv.2010.08.040, 2010.

Guenther, A., Karl, T., Harley, P., Wiedinmyer, C., Palmer, P. I., and Geron, C.: Estimates of global terrestrial isoprene emissions using MEGAN (Model of Emissions of Gases and Aerosols from Nature), *Atmos. Chem. Phys.*, 6, 3181–3210, doi:10.5194/acp-6-3181-2006, 2006.

Hallquist, M., Wenger, J. C., Baltensperger, U., Rudich, Y., Simpson, D., Claeys, M., Dommen, J., Donahue, N. M., George, C., Goldstein, A. H., Hamilton, J. F., Herrmann, H., Hoffmann, T., Iinuma, Y., Jang, M., Jenkin, M. E., Jimenez, J. L., Kiendler-Scharr, A., Maenhaut, W., McFiggans, G., Mentel, Th. F., Monod, A., Prévôt, A. S. H., Seinfeld, J. H., Suratt, J. D., Szmigielski, R., and Wildt, J.: The formation, properties and impact of secondary organic aerosol: current and emerging issues, *Atmos. Chem. Phys.*, 9, 5155–5236, doi:10.5194/acp-9-5155-2009, 2009.

Henry, K. M. and Donahue, N. M.: Photochemical aging of alpha-pinene secondary organic aerosol: effects of OH radical sources and photolysis, *J. Phys. Chem. A*, 116, 5932–5940, doi:10.1021/jp210288s, 2012.

Hinds, W. C.: *Aerosol Technology: Properties, Behavior, and Measurement of Airborne Particles*, John Wiley and Sons, New York, 1999.

Hu, D., Bian, Q., Li, T. W. Y., Lau, A. K. H., and Yu, J. Z.: Contributions of isoprene, monoterpenes, beta-caryophyllene, and toluene to secondary organic aerosols in Hong Kong during the summer of 2006, *J. Geophys. Res.-Atmos.*, 113, D22206, doi:10.1029/2008JD010437, 2008.

Iinuma, Y., Boge, O., Gnauk, T., and Herrmann, H.: Aerosol-chamber study of the alpha-pinene/O₃ reaction: influence of particle acidity on aerosol yields and products, *Atmos. Environ.*, 38, 761–773, doi:10.1016/j.atmosenv.2003.10.015, 2004.

Jaoui, M., Kleindienst, T. E., Lewandowski, M., Offenberg, J. H., and Edney, E. O.: Identification and quantification of aerosol polar oxygenated compounds bearing carboxylic or hydroxyl groups, 2. Organic tracer compounds from monoterpenes, *Environ. Sci. Technol.*, 39, 5661–5673, doi:10.1021/es048111b, 2005.

Temperature and
relative humidity
effects

J. Li et al.

- Jaoui, M., Edney, E. O., Kleindienst, T. E., Lewandowski, M., Offenberg, J. H., Surratt, J. D., and Seinfeld, J. H.: Formation of secondary organic aerosol from irradiated alpha-pinene/toluene/NO(x) mixtures and the effect of isoprene and sulfur dioxide, *J. Geophys. Res.-Atmos.*, 113, D09303, doi:10.1029/2007JD009426, 2008.
- 5 Kamens, R. M., Zhang, H., Chen, E. H., Zhou, Y., Parikh, H. M., Wilson, R. L., Galloway, K. E., and Rosen, E. P.: Secondary organic aerosol formation from toluene in an atmospheric hydrocarbon mixture: water and particle seed effects, *Atmos. Environ.*, 45, 2324–2334, 2011.
- 10 Kanakidou, M., Seinfeld, J. H., Pandis, S. N., Barnes, I., Dentener, F. J., Facchini, M. C., Van Dingenen, R., Ervens, B., Nenes, A., Nielsen, C. J., Swietlicki, E., Putaud, J. P., Balkanski, Y., Fuzzi, S., Horth, J., Moortgat, G. K., Winterhalter, R., Myhre, C. E. L., Tsigaridis, K., Vignati, E., Stephanou, E. G., and Wilson, J.: Organic aerosol and global climate modelling: a review, *Atmos. Chem. Phys.*, 5, 1053–1123, doi:10.5194/acp-5-1053-2005, 2005.
- Kawamura, K. and Ikushima, K.: Seasonal changes in the distribution of dicarboxylic acids in the urban atmosphere, *Environ. Sci. Technol.*, 27, 2227–2235, 1993.
- 15 Kawamura, K. and Pavuluri, C. M.: New directions: need for better understanding of plastic waste burning as inferred from high abundance of terephthalic acid in South Asian aerosols, *Atmos. Environ.*, 44, 5320–5321, doi:10.1016/j.atmosenv.2010.09.016, 2010.
- Kawamura, K. and Yasui, O.: Diurnal changes in the distribution of dicarboxylic acids, ketocarboxylic acids and dicarbonyls in the urban Tokyo atmosphere, *Atmos. Environ.*, 39, 1945–1960, doi:10.1016/j.atmosenv.2004.12.014, 2005.
- 20 Kawamura, K., Imai, Y., and Barrie, L. A.: Photochemical production and loss of organic acids in high Arctic aerosols during long-range transport and polar sunrise ozone depletion events, *Atmos. Environ.*, 39, 599–614, doi:10.1016/j.atmosenv.2004.10.020, 2005.
- Kleindienst, T. E.: Epoxying isoprene chemistry, *Science*, 325, 687–688, doi:10.1126/science.1178324, 2009.
- 25 Kleindienst, T. E., Edney, E. O., Lewandowski, M., Offenberg, J. H., and Jaoui, M.: Secondary organic carbon and aerosol yields from the irradiations of isoprene and alpha-pinene in the presence of NO_x and SO₂, *Environ. Sci. Technol.*, 40, 3807–3812, doi:10.1021/es052446r, 2006.
- 30 Kleindienst, T. E., Jaoui, M., Lewandowski, M., Offenberg, J. H., Lewis, C. W., Bhate, P. V., and Edney, E. O.: Estimates of the contributions of biogenic and anthropogenic hydrocarbons to secondary organic aerosol at a southeastern US location, *Atmos. Environ.*, 41, 8288–8300, doi:10.1016/j.atmosenv.2007.06.045, 2007.

Title Page	
Abstract	Introduction
Conclusions	References
Tables	Figures
◀	▶
◀	▶
Back	Close
Full Screen / Esc	
Printer-friendly Version	
Interactive Discussion	



Temperature and
relative humidity
effects

J. Li et al.

Title Page

Abstract

Introduction

Conclusions

References

Tables

Figures

◀

▶

Back

Close

Full Screen / Esc

Printer-friendly Version

Interactive Discussion



Kourtchev, I., Ruuskanen, T. M., Keronen, P., Sogacheva, L., Dal Maso, M., Reissell, A., Chi, X., Vermeylen, R., Kulmala, M., Maenhaut, W., and Claeys, M.: Determination of isoprene and α -/ β -pinene oxidation products in boreal forest aerosols from Hyttiälä, Finland: diel variations and possible link with particle formation events, *Plant Biol.*, 10, 138–149, doi:10.1055/s-2007-964945, 2008a.

Kourtchev, I., Warnke, J., Maenhaut, W., Hoffmann, T., and Claeys, M.: Polar organic marker compounds in PM_{2.5} aerosol from a mixed forest site in western Germany, *Chemosphere*, 73, 1308–1314, 2008b.

Kulmala, M., Asmi, A., Lappalainen, H. K., Baltensperger, U., Brenguier, J.-L., Facchini, M. C., Hansson, H.-C., Hov, Ø., O'Dowd, C. D., Pöschl, U., Wiedensohler, A., Boers, R., Boucher, O., de Leeuw, G., Denier van der Gon, H. A. C., Feichter, J., Krejci, R., Laj, P., Lihavainen, H., Lohmann, U., McFiggans, G., Mentel, T., Pilinis, C., Riipinen, I., Schulz, M., Stohl, A., Swietlicki, E., Vignati, E., Alves, C., Amann, M., Ammann, M., Arabas, S., Artaxo, P., Baars, H., Beddows, D. C. S., Bergström, R., Beukes, J. P., Bilde, M., Burkhardt, J. F., Canonaco, F., Clegg, S. L., Coe, H., Crumeyrolle, S., D'Anna, B., Decesari, S., Gilardoni, S., Fischer, M., Fjaeraa, A. M., Fountoukis, C., George, C., Gomes, L., Halloren, P., Hamburger, T., Harrison, R. M., Herrmann, H., Hoffmann, T., Hoose, C., Hu, M., Hyvärinen, A., Hörrak, U., Iinuma, Y., Iversen, T., Josipovic, M., Kanakidou, M., Kiendler-Scharr, A., Kirkevåg, A., Kiss, G., Klimont, Z., Kolmonen, P., Komppula, M., Kristjánsson, J.-E., Laakso, L., Laaksonen, A., Labonne, L., Lanz, V. A., Lehtinen, K. E. J., Rizzo, L. V., Makkonen, R., Manninen, H. E., McMeeking, G., Merikanto, J., Minikin, A., Mirme, S., Morgan, W. T., Nemitz, E., O'Donnell, D., Panwar, T. S., Pawlowska, H., Petzold, A., Pienaar, J. J., Pio, C., Plass-Duelmer, C., Prévôt, A. S. H., Pryor, S., Reddington, C. L., Roberts, G., Rosenfeld, D., Schwarz, J., Selander, Ø., Sellegrí, K., Shen, X. J., Shiraiwa, M., Siebert, H., Sierau, B., Simpson, D., Sun, J. Y., Topping, D., Tunved, P., Vaattovaara, P., Vakkari, V., Veefkind, J. P., Visschedijk, A., Vuollekoski, H., Vuolo, R., Wehner, B., Wildt, J., Woodward, S., Worsnop, D. R., van Zadelhoff, G.-J., Zardini, A. A., Zhang, K., van Zyl, P. G., Kerminen, V.-M., Carslaw, K., and Pandis, S. N.: General overview: European Integrated project on Aerosol Cloud Climate and Air Quality interactions (EUCAARI) – integrating aerosol research from nano to global scales, *Atmos. Chem. Phys.*, 11, 13061–13143, doi:10.5194/acp-11-13061-2011, 2011.

Temperature and
relative humidity
effects

J. Li et al.

Title Page

Abstract

Introduction

Conclusions

References

Tables

Figures

◀

▶

Back

Close

Full Screen / Esc

Printer-friendly Version

Interactive Discussion



Lewandowski, M., Jaoui, M., Kleindienst, T. E., Offenberg, J. H., and Edney, E. O.: Composition of PM_{2.5} during the summer of 2003 in Research Triangle Park, North Carolina, *Atmos. Environ.*, 41, 4073–4083, 2007.

Li, J. J., Wang, G. H., Zhou, B. H., Cheng, C. L., Cao, J. J., Shen, Z. X., and An, Z. S.: Chemical composition and size distribution of wintertime aerosols in the atmosphere of Mt. Hua in central China, *Atmos. Environ.*, 45, 1251–1258, doi:10.1016/j.atmosenv.2010.12.009, 2011.

Li, J. J., Wang, G. H., Zhou, B. H., Cheng, C. L., Cao, J. J., Shen, Z. X., and An, Z. S.: Airborne particulate organic markers at the summit (2060 m, a.s.l.) of Mt. Hua in central China during winter: implications for biofuel and coal combustion, *Atmos. Res.*, 106, 108–119, 2012.

Li, J. J., Wang, G. J., Wang, X. M., Cao, J. J., Sun, T., Cheng, C. L., Meng, J. J., Hu, T. F., and Liu, S. X.: Abundance, composition and source of atmospheric PM_{2.5} at a remote site in Tibetan Plateau, China, *Tellus B*, under review, 2013.

Lin, Y. H., Zhang, Z. F., Docherty, K. S., Zhang, H. F., Budisulistiorini, S. H., Rubitschun, C. L., Shaw, S. L., Knipping, E. M., Edgerton, E. S., Kleindienst, T. E., Gold, A., and Surratt, J. D.: Isoprene epoxydiols as precursors to secondary organic aerosol formation: acid-catalyzed reactive uptake studies with authentic compounds, *Environ. Sci. Technol.*, 46, 250–258, doi:10.1021/es202554c, 2012.

Lin, Y.-H., Zhang, H., Pye, H. O. T., Zhang, Z., Marth, W. J., Park, S., Arashiro, M., Cui, T., Budisulistiorini, S. H., Sexton, K. G., Vizuete, W., Xie, Y., Luecken, D. J., Piletic, I. R., Edney, E. O., Bartolotti, L. J., Gold, A., and Surratt, J. D.: Epoxide as a precursor to secondary organic aerosol formation from isoprene photooxidation in the presence of nitrogen oxides, *P. Natl. Acad. Sci. USA*, 110, 6718–6723, doi:10.1073/pnas.1221150110, 2013a.

Lin, Y.-H., Knipping, E. M., Edgerton, E. S., Shaw, S. L., and Surratt, J. D.: Investigating the influences of SO₂ and NH₃ levels on isoprene-derived secondary organic aerosol formation using conditional sampling approaches, *Atmos. Chem. Phys. Discuss.*, 13, 3095–3134, doi:10.5194/acpd-13-3095-2013, 2013b.

Nguyen, T. B., Roach, P. J., Laskin, J., Laskin, A., and Nizkorodov, S. A.: Effect of humidity on the composition of isoprene photooxidation secondary organic aerosol, *Atmos. Chem. Phys.*, 11, 6931–6944, doi:10.5194/acp-11-6931-2011, 2011.

Offenberg, J. H., Lewandowski, M., Edney, E. O., Kleindienst, T. E., and Jaoui, M.: Influence of Aerosol Acidity on the Formation of Secondary Organic Aerosol from Biogenic Precursor Hydrocarbons, *Environ. Sci. Technol.*, 43, 7742–7747, doi:10.1021/es901538e, 2009.

Temperature and relative humidity effects

J. Li et al.

Offenberg, J. H., Lewandowski, M., Jaoui, M., and Kleindienst, T. E.: Contributions of biogenic and anthropogenic hydrocarbons to secondary organic aerosol during 2006 in Research Triangle Park, NC, *Aerosol Air Qual. Res.*, 11, 99–U15, doi:10.4209/aaqr.2010.11.0102, 2011.

Shen, Z. X., Arimoto, R., Cao, J. J., Zhang, R. J., Li, X. X., Du, N., Okuda, T., Nakao, S., and Tanaka, S.: Seasonal variations and evidence for the effectiveness of pollution controls on water-soluble inorganic species in total suspended particulates and fine particulate matter from Xi'an, China, *J. Air Waste Manage.*, 58, 1560–1570, doi:10.3155/1047-3289.58.12.1560, 2008.

Simoneit, B. R. T., Elias, V. O., Kobayashi, M., Kawamura, K., Rushdi, A. I., Medeiros, P. M., Rogge, W. F., and Didyk, B. M.: Sugars – dominant water-soluble organic compounds in soils and characterization as tracers in atmospheric particulate matter, Environ. Sci. Technol., 38, 5939–5949, doi:10.1021/es0403099, 2004a.

Simoneit, B. R. T., Kobayashi, M., Mochida, M., Kawamura, K., and Huebert, B. J.: Aerosol particles collected on aircraft flights over the northwestern Pacific region during the ACE-Asia campaign: composition and major sources of the organic compounds, *J. Geophys. Res.-Atmos.*, 109, D19S09, doi:10.1029/2004JD004565, 2004b.

Stone, E. A., Hedman, C. J., Zhou, J., Mieritz, M., and Schauer, J. J.: Insights into the nature of secondary organic aerosol in Mexico City during the MILAGRO experiment 2006, *Atmos. Environ.*, 44, 312–319, 2010.

Surratt, J. D., Chan, A. W. H., Eddingsaas, N. C., Chan, M. N., Loza, C. L., Kwan, A. J., Hersey, S. P., Flagan, R. C., Wennberg, P. O., and Seinfeld, J. H.: Reactive intermediates revealed in secondary organic aerosol formation from isoprene, *P. Natl. Acad. Sci. USA*, 107, 6640–6645, doi:10.1073/pnas.0911114107, 2010.

Szmigelski, R., Surratt, J. D., Gomez-Gonzalez, Y., Van der Veken, P., Kourtchev, I., Vermeylen, R., Blockhuys, F., Jaoui, M., Kleindienst, T. E., Lewandowski, M., Offenberg, J. H., Edney, E. O., Seinfeld, J. H., Maenhaut, W., and Claeys, M.: 3-methyl-1,2,3-butanetricarboxylic acid: an atmospheric tracer for terpene secondary organic aerosol, *Geophys. Res. Lett.*, 34, L24811, doi:10.1029/2007GL031338, 2007.

Turpin, B. J. and Huntzicker, J. J.: Identification of secondary organic aerosol episodes and quantitation of primary and secondary organic aerosol concentrations during SCAQS, Atmos. Environ., 29, 3527–3544, 1995.

van Donkelaar, A., Martin, R. V., Brauer, M., Kahn, R., Levy, R., Verduzco, C., and Vileneuve, P. J.: Global estimates of ambient fine particulate matter concentrations from

Title Page

Abstract

Introduction

Conclusions

References

Tables

Figures

1

1

1

A small blue triangle icon pointing to the right, located at the bottom right corner of the slide.

Back

Close

Full Screen / Esc

[Printer-friendly Version](#)

Interactive Discussion



Temperature and relative humidity effects

J. Li et al.

[Title Page](#)[Abstract](#)[Introduction](#)[Conclusions](#)[References](#)[Tables](#)[Figures](#)[◀](#)[▶](#)[◀](#)[▶](#)[Back](#)[Close](#)[Full Screen / Esc](#)[Printer-friendly Version](#)[Interactive Discussion](#)

- satellite-based aerosol optical depth: development and application, *Environ. Health Persp.*, 118, 847–855, doi:10.1289/ehp.0901623, 2010.
- Wang, G., Kawamura, K., Xie, M., Hu, S., Gao, S., Cao, J., An, Z., and Wang, Z.: Size-distributions of *n*-alkanes, PAHs and hopanes and their sources in the urban, mountain and marine atmospheres over East Asia, *Atmos. Chem. Phys.*, 9, 8869–8882, doi:10.5194/acp-9-8869-2009, 2009.
- Wang, G., Xie, M., Hu, S., Gao, S., Tachibana, E., and Kawamura, K.: Dicarboxylic acids, metals and isotopic compositions of C and N in atmospheric aerosols from inland China: implications for dust and coal burning emission and secondary aerosol formation, *Atmos. Chem. Phys.*, 10, 6087–6096, doi:10.5194/acp-10-6087-2010, 2010.
- Wang, G. H., Kawamura, K., Lee, S., Ho, K. F., and Cao, J. J.: Molecular, seasonal, and spatial distributions of organic aerosols from fourteen Chinese cities, *Environ. Sci. Technol.*, 40, 4619–4625, doi:10.1021/es060291x, 2006.
- Wang, G. H., Kawamura, K., Hatakeyama, S., Takami, A., Li, H., and Wang, W.: Aircraft measurement of organic aerosols over China, *Environ. Sci. Technol.*, 41, 3115–3120, doi:10.1021/es062601h, 2007.
- Wang, G. H., Chen, C. L., Li, J. J., Zhou, B. H., Xie, M. J., Hu, S. Y., Kawamura, K., and Chen, Y.: Molecular composition and size distribution of sugars, sugar-alcohols and carboxylic acids in airborne particles during a severe urban haze event caused by wheat straw burning, *Atmos. Environ.*, 45, 2473–2479, doi:10.1016/j.atmosenv.2011.02.045, 2011.
- Wang, G. H., Kawamura, K., Cheng, C. L., Li, J. J., Cao, J. J., Zhang, R. J., Zhang, T., Liu, S. X., and Zhao, Z. Z.: Molecular distribution and stable carbon isotopic composition of dicarboxylic acids, ketocarboxylic acids, and alpha-dicarbonyls in size-resolved atmospheric particles from Xi'an City, China, *Environ. Sci. Technol.*, 46, 4783–4791, doi:10.1021/es204322c, 2012.
- Wang, W., Wu, M. H., Li, L., Zhang, T., Liu, X. D., Feng, J. L., Li, H. J., Wang, Y. J., Sheng, G. Y., Claeys, M., and Fu, J. M.: Polar organic tracers in PM_{2.5} aerosols from forests in eastern China, *Atmos. Chem. Phys.*, 8, 7507–7518, doi:10.5194/acp-8-7507-2008, 2008.
- Xue, J., Lau, A. K. H., and Yu, J. Z.: A study of acidity on PM_{2.5} in Hong Kong using online ionic chemical composition measurements, *Atmos. Environ.*, 45, 7081–7088, doi:10.1016/j.atmosenv.2011.09.040, 2011.
- Zhang, H., Surratt, J. D., Lin, Y. H., Bapati, J., and Kamens, R. M.: Effect of relative humidity on SOA formation from isoprene/NO photooxidation: enhancement of 2-methylglyceric acid and

its corresponding oligoesters under dry conditions, *Atmos. Chem. Phys.*, 11, 6411–6424, doi:10.5194/acp-11-6411-2011, 2011.

Zhang, Y. Y., Müller, L., Winterhalter, R., Moortgat, G. K., Hoffmann, T., and Pöschl, U.: Seasonal cycle and temperature dependence of pinene oxidation products, dicarboxylic acids and nitrophenols in fine and coarse air particulate matter, *Atmos. Chem. Phys.*, 10, 7859–7873, doi:10.5194/acp-10-7859-2010, 2010.

Zhou, Y., Zhang, H., Parikh, H. M., Chen, E. H., Rattanavaraha, W., Rosen, E. P., Wang, W., and Kamens, R. M.: Secondary organic aerosol formation from xylenes and mixtures of toluene and xylenes in an atmospheric urban hydrocarbon mixture: water and particle seed effects (II), *Atmos. Environ.*, 45, 3882–3890, 2011.

ACPD

13, 17643–17674, 2013

Temperature and
relative humidity
effects

J. Li et al.

Title Page

Abstract

Introduction

Conclusions

References

Tables

Figures



Back

Close

Full Screen / Esc

Printer-friendly Version

Interactive Discussion





Table 1. Chemical character and possible source of detected organic markers.

Order	Organic marker	Chemical structure	Molecular formula	Molecular weight	<i>m/z</i> ^a	Possible source
1	Succinic acid (C_4^{di}) ^b		$C_4H_6O_4$	118	247	Photochemical product of unsaturated hydrocarbons and fatty acids; direct emission from coal and biomass burning.
2	2-Methylglyceric acid (MGA) ^b		$C_5H_8O_4$	120	103	Photochemical product of isoprene.
3	Glutaric acid (C_5^{di})		$C_5H_8O_4$	132	147	Photochemical product of unsaturated hydrocarbons and fatty acids; direct emission from coal and biomass burning.
4	Malic acid (MA)		$C_4H_6O_5$	134	147	Photochemical product of unsaturated hydrocarbons and fatty acids; direct emission from coal and biomass burning.
5	<i>cis</i> -Pinonic acid (PA)		$C_{10}H_{16}O_3$	184	171	Photochemical product of monoterpene.
6	2-Methylthreitol (MT)		$C_5H_{12}O_4$	136	147	Photochemical product of isoprene.
7	2-Methylerythritol (ME)		$C_5H_{12}O_4$	136	147	Photochemical product of isoprene.
8	3-Hydroxyglutaric acid (HGA)		$C_5H_8O_5$	148	147	Photochemical product of monoterpene.
9	<i>o</i> -Phthalic acid (<i>o</i> -Ph)		$C_8H_8O_4$	166	295	Photochemical product of toluene, xylene, naphthalene and other anthropogenic pollutants.
10	Levoglucosan (Levo)		$C_6H_{10}O_5$	162	217	Pyrolysis product of materials containing cellulose.
11	Arabitol (Arab)		$C_5H_{12}O_5$	152	217	Direct emission by microorganism, plants and animals.
12	3-Methyl-1,2,3-butane tricarboxylic acid (MBTCA)		$C_8H_{12}O_6$	204	147	Photochemical product of monoterpene.
13	<i>m</i> -Phthalic acid (<i>m</i> -Ph)		$C_8H_8O_4$	166	295	Photochemical product of toluene, xylene, naphthalene and other anthropogenic pollutants.
14	<i>p</i> -Phthalic acid (<i>p</i> -Ph)		$C_8H_8O_4$	166	295	Direct emission by open burning of new plastic bags, roadside litter and landfill trash; secondary formation.
15	β -Caryophyllinic acid		$C_{14}H_{22}O_4$	254	383	Photochemical product of β -caryophyllene.

^a Mass-to-charge ratio of fragment ions for qualification and quantification.

Table 2. Concentrations (ng m^{-3}) of biogenic secondary organic aerosols and other compounds in PM_{10} of Mt. Hua.

	Southerly ($N = 17$) ^a	Easterly ($N = 11$) ^a	Northerly ($N = 6$) ^a	Average ($N = 34$)
T (°C)	18 ± 2.1	16 ± 1.1	18 ± 2.2	17 ± 2.1
RH (%)	85 ± 10	91 ± 5.0	64 ± 13	84 ± 13
PM_{10} ($\mu\text{g m}^{-3}$)	42 ± 17	42 ± 17	46 ± 6.6	43 ± 17
OC ($\mu\text{g m}^{-3}$)	4.0 ± 1.2	3.0 ± 1.2	3.0 ± 0.87	3.5 ± 1.3
EC ($\mu\text{g m}^{-3}$)	0.65 ± 0.26	0.57 ± 0.20	0.78 ± 0.37	0.65 ± 0.27
SO_4^{2-} ($\mu\text{g m}^{-3}$)	19 ± 9.9	23 ± 11	15 ± 6.8	21 ± 12
NO_3^- ($\mu\text{g m}^{-3}$)	1.2 ± 1.7	1.5 ± 1.3	2.0 ± 0.4	1.4 ± 1.4
NH_4^+ ($\mu\text{g m}^{-3}$)	4.0 ± 2.0	5.1 ± 2.5	3.1 ± 1.4	4.3 ± 2.5
pH _{IS}	0.0 ± 0.55	0.30 ± 0.39	-1.08 ± 0.47	-0.08 ± 0.64
LWC ^b ($\mu\text{mol m}^{-3}$)	4.85 ± 5.27	7.01 ± 4.51	0.93 ± 0.34	4.87 ± 4.90
I. Isoprene derived SOA				
2-methylglyceric acid	4.7 ± 1.7	3.9 ± 2.4	2.7 ± 1.7	4.1 ± 2.2
2-methylthreitol	5.1 ± 2.9	2.4 ± 1.8	1.5 ± 1.2	3.6 ± 2.8
2-methylerythritol	6.7 ± 3.5	3.7 ± 3.1	2.6 ± 1.8	4.9 ± 3.6
subtotal	16 ± 7.6	10 ± 6.9	6.8 ± 4.7	13 ± 8.2
$\text{SOC}_{\text{isoprene}}$ (ng C m^{-3}) ^c	106 ± 49	65 ± 45	44 ± 30	81 ± 53
II. α-/β-pinene derived SOA				
cis-pinonic acid	3.3 ± 1.4	2.5 ± 1.1	3.1 ± 1.4	3.0 ± 1.4
3-hydroxyglutaric acid	2.6 ± 1.1	1.6 ± 0.78	1.4 ± 0.67	2.1 ± 1.1
MBTCA	2.2 ± 1.1	1.0 ± 0.64	0.88 ± 0.49	1.6 ± 1.1
subtotal	8.1 ± 3.1	5.1 ± 2.3	5.3 ± 2.4	6.6 ± 3.3
$\text{SOC}_{\text{pinene}}$ (ng C m^{-3}) ^c	35 ± 13	22 ± 9.8	23 ± 10	29 ± 14
III. β-caryophyllene derived SOA				
β -caryophyllinic acid	2.7 ± 1.1	1.9 ± 1.0	2.3 ± 1.6	2.2 ± 1.2
$\text{SOC}_{\text{caryophyllene}}$ (ng C m^{-3}) ^c	116 ± 47	81 ± 42	98 ± 72	98 ± 53
IV. Other organic compounds				
Succinic acid	6.7 ± 3.1	6.8 ± 3.5	1.6 ± 0.41	5.8 ± 3.6
Glutamic acid	2.4 ± 1.0	2.2 ± 1.3	0.88 ± 0.31	2.2 ± 1.5
Malic acid	7.3 ± 2.4	5.1 ± 2.6	2.7 ± 1.5	5.8 ± 3.2
α -Phthalic acid	6.2 ± 2.3	4.4 ± 2.1	2.9 ± 1.5	4.9 ± 2.5
m -Phthalic acid	0.18 ± 0.08	0.13 ± 0.06	0.15 ± 0.08	0.16 ± 0.08
p -Phthalic acid	2.7 ± 2.2	1.7 ± 1.7	3.0 ± 3.0	2.3 ± 2.2
Levoglucosan	17 ± 13	12 ± 12	14 ± 6.8	14 ± 12
Arabitol	6.1 ± 4.0	4.3 ± 2.8	5.9 ± 0.63	5.5 ± 3.5

^a Mean concentrations of detected compounds in PM_{10} of Mt. Hua from southerly, easterly and northerly air masses based on back-trajectories analysis.

^b LWC: liquid water content in the aqueous phase of PM_{10} .

^c The total mass concentrations of SOC (secondary organic carbon) produced by isoprene, α -/ β -pinene, and β -caryophyllene were calculated using a tracer-based method reported by Kleindienst et al. (2007).

Temperature and relative humidity effects

J. Li et al.

Title Page

Abstract

Introduction

Conclusions

References

Tables

Figures

◀

▶

Back

Close

Full Screen / Esc

Printer-friendly Version

Interactive Discussion



Temperature and relative humidity effects

J. Li et al.

Table 3. Comparison of biogenic secondary organic aerosol tracers in the Mt. Hua aerosols with those reported by other studies during summer.

Location	Latitude (°)	Aerosols type	Isoprene products	α -/ β -pinene products	β -caryophyllene products	2-methyltetrols -C/OC (%)	$R_{MBTCA/PA}$	Reference
Changbai, China	42°24' N	PM _{2.5}	53	31	NA ^a	0.45	NA	Wang et al. (2008)
Mt. Tai, China	36°41' N	TSP	171	30	12	0.32	1.0	Fu et al. (2010)
Mt. Hu, China	34°29' N	PM ₁₀	13	6.6	2.2	0.11	0.54	This study
Chongming, China	30°50' N	PM _{2.5}	48	1.8	NA	0.02	NA	Wang et al. (2008)
Dinghu, China	23°10' N	PM _{2.5}	26	NA	NA	0.17	NA	Wang et al. (2008)
Wangqingsha, China	22°42' N	PM _{2.5}	31	6.6	0.54	0.07	0.32	Ding et al. (2011)
Hong Kong, China	22°13' N	PM _{2.5}	30	198	13	0.24	NA	Hu et al. (2008)
Hainan, China	18°40' N	PM _{2.5}	51	9.4	NA	0.75	NA	Wang et al. (2008)
Alert, Canada	82°30' N	TSF	0.30	1.6	0.12	0.02	9.4	Fu et al. (2009)
Hyttälä, Finland	61°51' N	PM ₁	17	65	NA	0.25	NA	Kourtchev et al. (2008a)
Jülich, Germany	50°54' N	PM _{2.5}	21	26	NA	0.14	NA	Kourtchev et al. (2008b)
RTP, NC, USA	35°54' N	PM _{2.5}	137	153	11	NA	NA	Lewandowski et al. (2007)
An urban site in Mexico	19°29' N	PM _{2.5}	34	48	3.4	0.17	0.91	Stone et al. (2010)
A rural site in Mexico	19°42' N	PM _{2.5}	32	55	5.7	0.28	4.8	Stone et al. (2010)
Balbina, Brazil	1°55' S	PM _{2.5}	57	NA	NA	1.8	NA	Claeys et al. (2004)

^a NA; not available.



Temperature and relative humidity effects

J. Li et al.

[Title Page](#)[Abstract](#)[Introduction](#)[Conclusions](#)[References](#)[Tables](#)[Figures](#)[◀](#)[▶](#)[◀](#)[▶](#)[Back](#)[Close](#)[Full Screen / Esc](#)[Printer-friendly Version](#)[Interactive Discussion](#)**Table 4.** Concentration (ng m^{-3}) and geometric mean diameters (GMD, μm) of BSOA and other components in fine ($< 2.1 \mu\text{m}$) and coarse modes ($> 2.1 \mu\text{m}$).

	Fine mode ($< 2.1 \mu\text{m}$)		Coarse mode ($> 2.1 \mu\text{m}$)	
	Concentration	GMD ^a	Concentration	GMD ^a
Particle mass ($\mu\text{g m}^{-3}$)	26 ± 3.7	0.82 ± 0.01	20 ± 3.9	9.82 ± 1.27
SO_4^{2-} ($\mu\text{g m}^{-3}$)	11 ± 1.4	0.89 ± 0.03	3.0 ± 0.18	10.0 ± 1.51
NO_3^- ($\mu\text{g m}^{-3}$)	0.81 ± 0.45	0.58 ± 0.17	1.2 ± 0.32	9.41 ± 2.06
NH_4^+ ($\mu\text{g m}^{-3}$)	2.4 ± 0.51	0.90 ± 0.04	0.04 ± 0.01	5.97 ± 2.01
I. Isoprene derived SOA				
MGA	2.3 ± 0.54	0.87 ± 0.01	1.3 ± 0.27	8.77 ± 2.68
MT	3.4 ± 0.24	0.79 ± 0.06	1.3 ± 0.37	7.02 ± 1.88
ME	6.8 ± 1.09	0.82 ± 0.03	2.0 ± 0.56	6.38 ± 1.52
II. α -/ β -pinene derived SOA				
PA	1.6 ± 0.57	0.74 ± 0.03	2.4 ± 0.81	8.40 ± 2.81
HGA	1.6 ± 0.32	0.77 ± 0.02	ND ^b	ND ^b
MBTCA	1.5 ± 0.30	0.80 ± 0.04	0.05 ± 0.01	2.70 ± 0.00
III. β -caryophyllene derived SOA				
CA	1.2 ± 0.10	0.79 ± 0.01	ND ^b	ND ^b
III. Other organic compounds				
C_4^{di}	4.9 ± 0.97	0.98 ± 0.02	12.0 ± 0.54	9.96 ± 2.76
C_5^{di}	1.5 ± 0.11	0.88 ± 0.04	0.62 ± 0.17	9.22 ± 2.93
MA	5.5 ± 0.95	0.82 ± 0.04	0.47 ± 0.15	9.12 ± 3.70
<i>o</i> -P	4.6 ± 0.87	0.76 ± 0.03	4.3 ± 1.8	9.76 ± 3.11
<i>m</i> -P	0.11 ± 0.01	0.73 ± 0.04	0.04 ± 0.01	8.97 ± 3.19
<i>p</i> -P	1.8 ± 0.44	0.72 ± 0.06	0.38 ± 0.22	9.52 ± 5.94
Levo	11 ± 1.1	0.63 ± 0.05	1.3 ± 0.11	6.83 ± 2.28
Arab	0.32 ± 0.06	0.68 ± 0.08	7.1 ± 1.34	8.21 ± 2.78

^a $\log \text{GMD} = (\sum C_i \log D_{p,i}) / \sum C_i$, where C_i is the concentration of compound in size i and $D_{p,i}$ is the geometric mean particle diameter collected on stage i (Hinds, 1999).^b ND: not detected.

**Temperature and
relative humidity
effects**

J. Li et al.

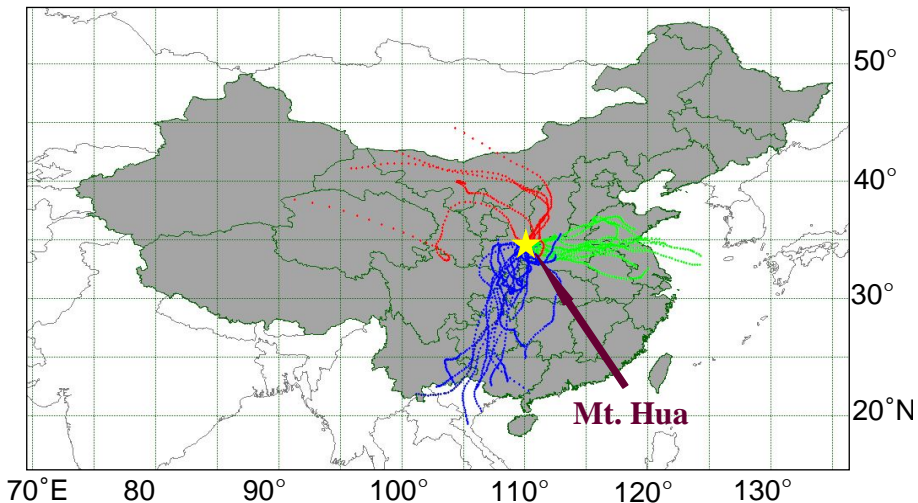


Fig. 1. Location of the sampling site (Mt. Hua; 34°29' N, 110°05' E; 2060 m.a.s.l.) and 72 h backward air mass trajectories reaching the summit during the sampling in the summer of 2009.

[Title Page](#)[Abstract](#)[Introduction](#)[Conclusions](#)[References](#)[Tables](#)[Figures](#)[Back](#)[Close](#)[Full Screen / Esc](#)[Printer-friendly Version](#)[Interactive Discussion](#)

Temperature and relative humidity effects

J. Li et al.

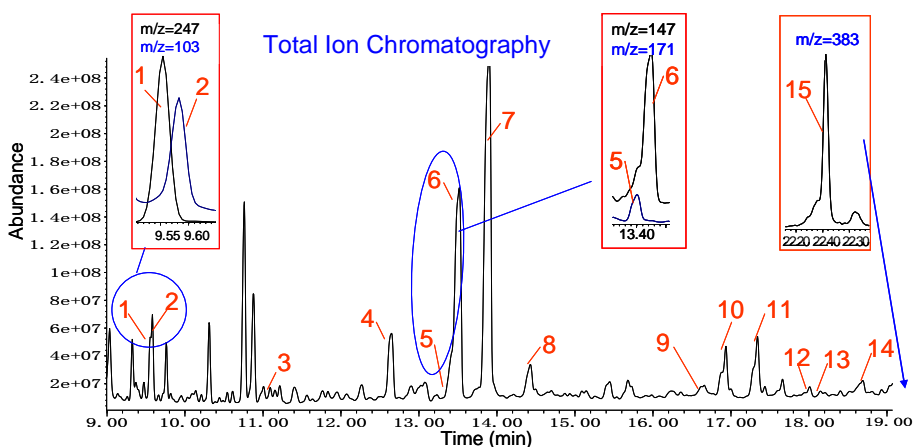


Fig. 2. GC/MS ion chromatography obtained for a trimethylsilylated PM₁₀ sample collected on 15 August 2009 (1. succinic acid; 2. 2-methylglyceric acid; 3. glutaric acid; 4. malic acid; 5. *cis*-pinonic acid; 6. 2-methylthreitol; 7. 2-methylerythritol; 8. 3-hydorxyglutaric acid; 9. *o*-phthalic acid; 10. levoglucosan; 11. arabitol; 12. 3-methyl-1,2,3-butanetricarboxylic acid; 13. *m*-phthalic acid; 14. *p*-phthalic acid; 15. β -caryophyllinic acid).

Title Page

Abstract

Introduction

Conclusion

References

Table

Figures



Temperature and relative humidity effects

J. Li et al.

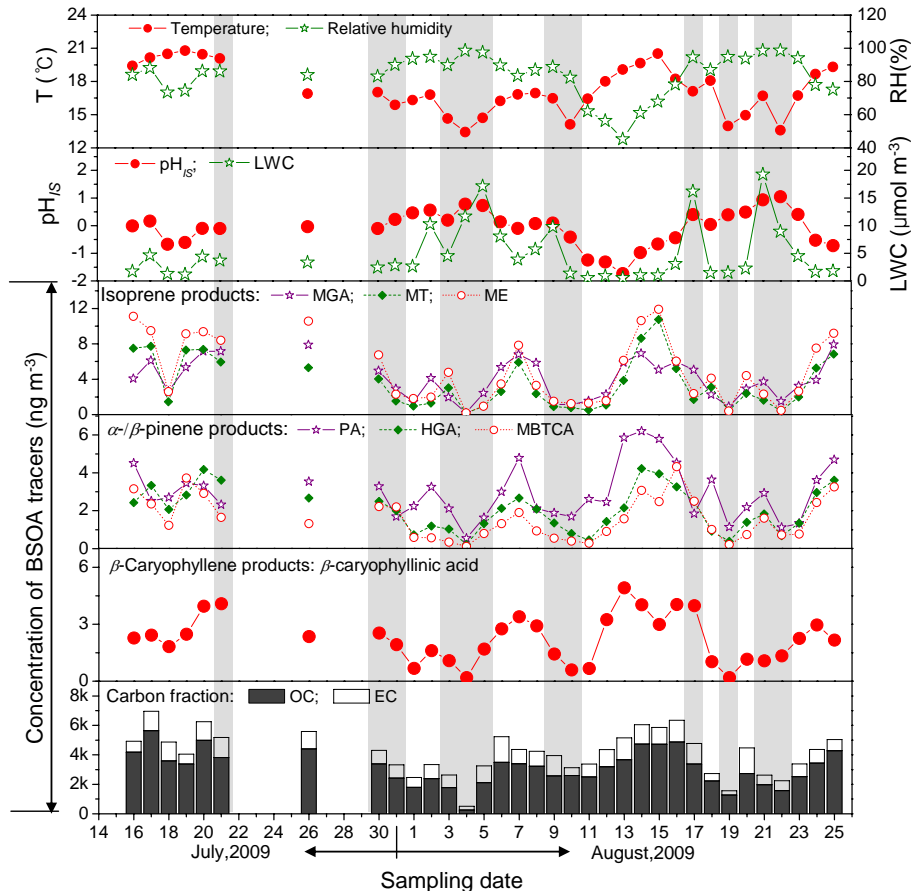


Fig. 3. Temporal variation of biogenic products as well as temperature, relative humidity, pH_{IS} (in-situ acidity of particles), LWC (liquid water content of particles), OC and EC (organic and elemental carbon). The shadows denote rainy periods.

Temperature and relative humidity effects

J. Li et al.

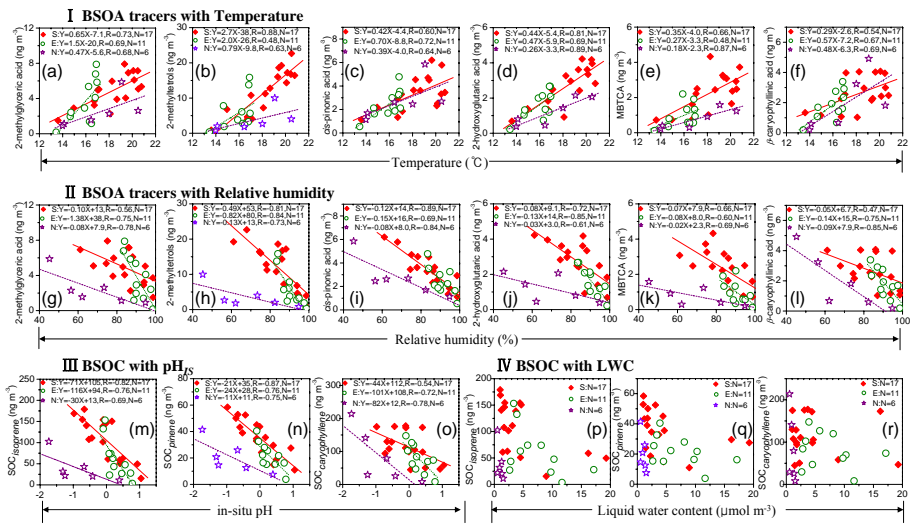


Fig. 4. Linear regression of (a–f) BSOA tracers with temperature, (g–l) BSOA tracers with relative humidity, (m–o) BSOC with in-situ pH (pH_{IS}), and (p–r) BSOC with liquid water content (LWC). S, E, N: the PM_{10} samples in Mt. Hua from southerly (S), easterly (E) and northerly (N) air masses. 2-methyltetrols: the sum of 2-methylthreitol and 2-methylerythritol; MBTCA: 3-methyl-1,2,3-butanetricarboxylic acid. SOC_{isoprene}, SOC_{pinene} and SOC_{caryophyllene}: the total mass concentrations of SOC (secondary organic carbon) produced by isoprene, α -/ β -pinene, and β -caryophyllene were calculated using a tracer-based method reported by Kleindienst et al. (2007).

Temperature and relative humidity effects

J. Li et al.

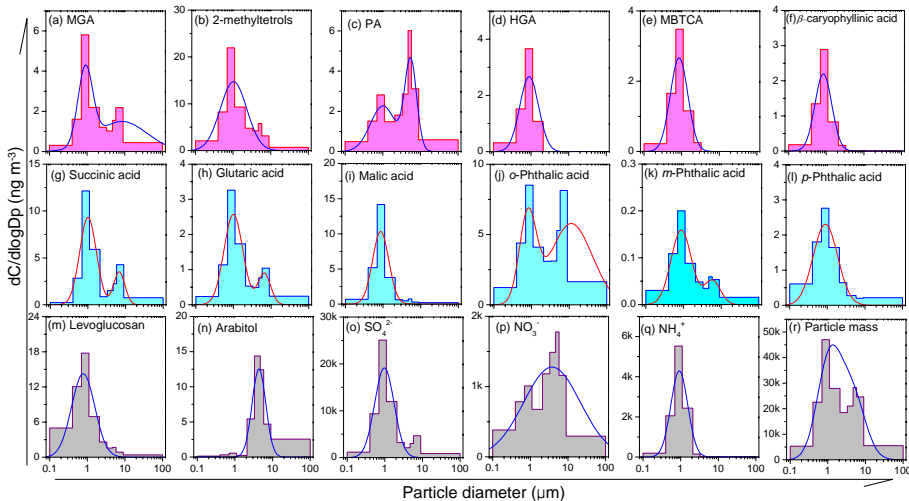


Fig. 5. Size distribution of (a–n) organic aerosols, (o–p) inorganic ions, and (r) particle mass (MGA: 2-methylglyceric acid, 2-methyltetrols: the sum of 2-methylthreitol and 2-methylerythritol; PA: *cis*-pinonic acid, HGA: 3-hydroxyglutaric acid, MBTCA: 2-methyl-1,2,3-butanetricarboxylic acid).